Published in final edited form as:
Biochim Biophys Acta. 2013 April ; 1833(4): 804–811. doi:10.1016/j.bbamcr.2012.08.011.

Impact of titin isoform on length dependent activation and cross-bridge cycling kinetics in rat skeletal muscle

Ryan D. Mateja[1,2], **Marion L. Greaser**[3], and **Pieter P. de Tombe**[1,2,*]

[1]Department of Cell and Molecular Physiology, Stritch School of Medicine, Loyola University medical Center, Maywood, Illinois 60153

[2]Department of Physiology and Biophysics, University of Illinois College of Medicine, Chicago Illinois 60612

[3]Department of Animal Sciences, Muscle Biology Laboratory, University of Wisconsin, Madison, Wisconsin 53711

Abstract

The magnitude of length dependent activation in striated muscle has been shown to vary with titin isoform. Recently, a rat that harbors a homozygous autosomal mutation (HM) causing preferential expression of a longer, giant titin isoform was discovered (Greaser et al. 2005). Here, we investigated the impact of titin isoform on myofilament force development and cross-bridge cycling kinetics as function of sarcomere length (SL) in tibialis anterior skeletal muscle isolated from wild type (WT) and HM. Skeletal muscle bundles from HM rats exhibited reductions in passive tension, maximal force development, myofilament calcium sensitivity, maximal ATP consumption, and tension cost at both short and long sarcomere length (SL=2.8 μm and SL=3.2 μm, respectively). Moreover, the SL-dependent changes in these parameters were attenuated in HM muscles. Additionally, myofilament Ca^{2+} activation-relaxation properties were assessed in single isolated myofibrils. Both the rate of tension generation upon Ca^{2+} activation (k_{ACT}) as well as the rate of tension redevelopment following a length perturbation (k_{TR}) were reduced in HM myofibrils compared to WT, while relaxation kinetics were not affected. We conclude that presence of a long isoform of titin in the striated muscle sarcomere is associated with reduced myofilament force development and cross-bridge cycling kinetics, and a blunting of myofilament length dependent activation.

Keywords

Titin; Myofilament Length Dependent Activation; Sarcomere Length; Actin-Myosin Interaction

1. Introduction

Spanning each half sarcomere from the Z disk to the M band, titin is the largest and third most abundant protein in mammalian striated muscle[1–5]. Additionally, because adjacent

*Address for Correspondence: Pieter P. de Tombe, Ph.D., Department of Cell and Molecular Physiology, Loyola University Chicago, 2160 South First Ave., Stritch School of Medicine, Maywood, IL 60153-5500, (708) 216-1018, (708) 216-6308 (FAX), pdetombe@lumc.edu.

filaments overlap in both the Z disk and the M band, titin effectively forms a continuous filament along an entire myofibril. The A-band region of titin is inextensible and contains super-repeats of immunoglobulin (Ig) and fibronectin type 3 (fn3) modules. The stretching of titin upon increases in sarcomere length (SL) occurs in the I-band region that includes extensible regions consisting of tandem arranged Ig-like domains, PEVK segments (rich in proline [P], glutamate [E], valine [V], and lysine [K]) and an N2 region (containing either N2B or N2A unique amino acid sequences). While it is expressed from a single gene, alternative splicing of titin mRNA in the I-band region allows for expression of different titin isoforms of varying size. Therefore, it is by altering the length of the extensible I-band regions that titin isoforms of varying stiffness are obtained.

The components, and therefore the length, of the middle Ig and PEVK sequence, largely differentiate titin isoforms[1–5]. Since titin acts as a “molecular spring” which provides a restoring force when a muscle is stretched, the longer titin isoforms causes muscles to have lower passive tension for a given change in SL than the shorter ones. Compared to cardiac muscle, skeletal muscles I-band region of titin is longer, causing it to produce much lower passive tension.

Due to the spanning the entire half sarcomere and having interactions with both the thick and thin filaments, titin is thought to play a role in myofilament length dependent activation. Length dependent activation (LDA) is characterized by an increase in maximal Ca^{2+} activated force and calcium sensitivity upon an increase in SL, which is particularly important in the heart where the mechanism underlies the Frank-Starling Law of the heart[6]. While the precise mechanism underlying LDA is unknown, many studies have shown that the amount of passive stiffness in a specific muscle type or preparation correlates to the amount of LDA exhibited[7–10]. This implicates titin as playing a pivotal role in myofilament length dependent activation since in skeletal and cardiac muscle, titin bears nearly all of the passive tension within physiological SL’s[1–5]. Furthermore, reducing the amount of passive tension carried by titin, either by specific degradation using trypsin or by modifying the muscle’s history dependence of stretch, has shown to greatly reduce or eliminate LDA[8, 11].

To investigate the contribution of titin based passive stiffness in LDA, here we utilized a rat that harbors a homozygous autosomal mutation (HM) causing preferential expression of a giant N2BA-G titin isoform. In the rat, titin undergoes developmental isoform changes; the longest isoforms are expressed during the embryonic stages and progressively get replaced by shorter isoforms[12, 13]. A recent investigation on the length of the titin isoforms in various muscles during development in both wild-type (WT) and HM rats showed that among all of the skeletal muscle examined in WT rats, the tibialis anterior (TA) undergoes the greatest extent of developmental shortening[14]. The TA titin isoform starts out at 3.7 MDa after birth, and by 180 days there are two shorter isoforms present, a 3.42 MDa isoform and a more abundant 3.29 MDa isoform. Due to the lack of normal developmental isoform shortening[13], HM rats maintain the much longer N2BA-G titin isoform in both the TA (3.7 MDa) and in the heart (3.8 MDa) [14, 15]. Accordingly, we investigated the SL dependence of Ca^{2+} activated force production and ATP consumption in both WT and HM TA skeletal muscle bundles. Furthermore, to examine the effect of titin isoform on cross-bridge cycling kinetics, we measured the rates of maximal activation and relaxation in WT and HM tibialis anterior myofibrils.

2. Materials and methods

2.1. Tissue procurement

All experiments were performed according to institutional guidelines concerning the care and use of experimental animals. The wild-type (WT) and homozygous mutant (HM) rats used in this study have been described previously[15–17]. Rats were anesthetized with sodium pentobarbital (50mg/kg i.p.) before removal of the left and right tibialis anterior muscle (TA). After removal, the TA was placed into a high potassium calcium free extracellular solution at 4°C and cut longitudinally into three or four smaller pieces (~3mm wide by ~20 mm strips). The strips were tied to small wooden sticks at physiological muscle length and placed in a 50% (v/v) glycerol/rigor solution at −20°C, which was replaced with fresh solution after 24 hours and stored at −20°C for up to 6 months.

2.1. Preparation of tibialis anterior fiber bundles and single myofibrils

TA fiber bundles were prepared by teasing away small bundles (0.1–0.25 mm wide by 1–2.5 mm long) from the larger aliquots under a dissection microscope in ice cold relaxing solution. The small bundles were stored for up to 3 days at 4°C in relaxing solution. Immediately prior to an experiment, bundles were crimped in aluminum T-clips in order to attach to hooks mounted on the force transducer and motor arm.

To prepare TA myofibrils, small strips of muscle (1mm wide by 10mm long) were dissected from the larger aliquots and then homogenized (9k rpm, 6 seconds) in ~1mL of relaxing solution on ice before being filtered (30 μm nylon filter) to remove large aggregates and debris. The HM tissue required slightly slower, but longer homogenization speeds (6k rpm, 12 seconds) to obtain good quality myofibrils, possibly due to the tissue having less mechanical stiffness related to the longer titin isoform. Myofibril preparations were then stored at 4°C and used for up to 4 days after preparation.

All solutions contained protease inhibitors (leupeptin, pepstatin, and PMSF) as well as a reducing compound (DTT). Furthermore, no differences in myofilament mechanical and energetic parameters were observed during the time of storage at 4 °C.

2.2. Simultaneous measurement of isometric tension and ATPase activity

The ATPase apparatus has been described previously[18, 19]. The skinned skeletal bundles were attached via aluminum T-clips between an optical force transducer (World Precision Instruments model KG4A; 0–20mN range 4μN resolution) and a high-speed length controller (Aurora Scientific Inc. model 315C; 200 microsecond step response time, 2.4 kHZ frequency response). The force transducer and length controller were mounted on a horizontal sliding arm that allowed for rapid translocation of the fiber between the different temperature controlled chambers on the apparatus. Isometric tension and ATP consumption were measured over a range of free Ca^{2+} concentrations as previously described[18, 19]. In addition, high frequency muscle length perturbation (1%; 500 Hz) were applied continuously to measure high frequency stiffness, an index we used to assess the relative number of attached actively cycling cross-bridges during tension development; there were no differences in stiffness relative to tension development under any condition or fiber bundle type (WT or HM) in the present study. Accordingly, it can be assumed that any differences in ATPase consumption rate were not due to changes in force generation per cycling cross-bridge[19]. ATP hydrolysis was stoichiometrically coupled to NADH consumption. Because NADH absorbs UV light (340 nm) and NAD^+ does not, ATP consumption can be determined by measurement of NADH light absorption. The method is illustrated in Figure 3; upon activation of the muscle by increasing the $[Ca^{2+}]$ in the bathing solution, UV light absorbance (proportional to [NADH]) decreases concomitant with the

development of muscle tension, reaching a steady state NADH consumption rate when muscle tension development stabilizes. Following removal of the muscle from the measurement chamber into a chamber containing relaxing solution, tension development relaxes and NADH consumption ceases. UV absorption is calibrated following each contraction by repeated injections of 500 pmol ADP into the measurement chamber (50 nl; 10 mM). SL was set to either 2.8 μm or 3.2 μm using laser diffraction; each fiber bundle underwent a series of activations at varying levels of free Ca^{2+} concentrations; the ATPase experiments were performed at 20°C.

2.3. Measurement of activation and relaxation kinetics in single myofibrils

The apparatus used for single myofibril activation-relaxation kinetics measurements has been described previously[20, 21]. Briefly, an aliquot of either WT or HM myofibril suspension in relaxing solution was injected into a chamber filled with ~2.5 mL bath relaxing solution that was mounted on the stage of an inverted microscope (Olympus IX-70). Myofibrils that were selected for use were attached horizontally between two glass tools, a custom-made black ink coated cantilever of known stiffness (acting as a force probe) and a rigid pipette attached to a piezo motor translation stage (Mad City Labs model Nano-driveOP30). Force was determined by measurement of the displacement of the force probe via edge detection, while SL was measured via FFT analysis of the myofibril striation pattern (IonOptix). Myofibrils were placed in one of the laminar solutions emanating from a double-barreled perfusion pipette; rapid translation of this pipette allowed for rapid switching between the two solutions. After a brief initial contraction to insure the myofibrils were attached appropriately, each myofibril underwent a single maximal saturated [Ca^{2+}] activation/relaxation cycle that included a 20% release-restretch maneuver during steady-state activation to determine (k_{TR}) [19, 22]. The rate of tension development following Ca^{2+} activation k_{ACT} and k_{TR} were determined by exponential fit; tension relaxation, which is biphasic under these conditions, was determined by both exponential and linear fits to the tension data[20, 21]. Myofibrils were studied at SL=2.8 μm and 15°C.

2.4. Titin isoform and myofilament protein expression

To determine titin isoform expression in both WT and HM TA muscle, TA homogenate samples were suspended in SDS sample buffer and underwent electrophoresis using vertical SDS agarose gels designed for high molecular weight protein separation as described previously[23]. Additionally, to assess the lower molecular weight myofilament protein isoform expression, homogenates samples were separated using standard SDS-PAGE (12%) [24]; gels were stained with Coomassie blue.

2.5. Solutions

The compositions of the activating and relaxing solutions were calculated according to the procedures developed by Fabiato as described previously[18]. Activating and relaxing solutions for myofibril experiments contained (in mmol/L): EGTA (1), MgATP (5), free Mg^{2+} (1), MOPS (10), Phosphocreatine (10). The pH was adjusted to 7.0 using KOH. Potassium Proprionate (Kprop) was added to adjust the final ionic strength to 180 mM. Contaminant P_i was reduced by adding the enzyme purine nucleoside phosphorylase with the substrate 7-methyl guanosine which acts as an P_i scavenging system[25]. A range of free [Ca^{2+}] was obtained by mixing activating solution (free [Ca^{2+}] = 0.1 mM) and relaxing solution (free [Ca^{2+}] ~ 1 nM). Bath solution was identical to relaxing solution except for the inclusion of 10 mM EGTA and the absence of the P_i scavenging system. All solutions contained protease inhibitors: leupeptin (10 μM), pepstatin (5 μM), phenylmethyl sulphonyl fluoride (200 μM), sodium azide (500 μM) and dithiothreitol (10 mM). The activating solution for the ATPase experiments contained (in mmol/L): $CaCl_2$ (10), EGTA (10), $MgCl_2$ (6.63), Kprop (14.28), ATP (6.29); the pre-activating solution contained (in mmol/L):

EGTA (0.2), HDTA (9.8), $MgCl_2$ (6.69), Kprop (34.35), ATP (6.2); the relaxing solution contained (in mmol/L): EGTA (10), $MgCl_2$ (6.92), Kprop (33.99), ATP (6.2). In addition, all three solutions contained (in mmol/L): BES (100), NaN_3 (5), PEP (10), DTT (1), NADH (0.9), Pepstatin (1); and (in μmol/L): Leupeptin (10), PMSF (100), Oligomycin (10), A2P5 (20), and the enzymes Pyruvate Kinase (4 mg/mL;500 U/mg) and Lactate Dehydrogenase (0.24mg/mL;870 U/mg). Solutions were adjusted to pH 7.0 using KOH. Calcium free extracellular solution contained (in mmol/L): TRIS (50), NaCl (100), KCl (2), $MgCl_2$(2), EGTA (1). The pH was adjusted to 7.0 using HCl. Rigor solution contained (in mmol/L): TRIS (50), KCl (100), $MgCl_2$ (2), EGTA (1); pH was adjusted to 7.0 using HCl.

2.6. Data Processing and Statistical Analysis

Data were fit for each muscle or myofibril preparation individually; fit parameters were next used for calculation of average values and statistics. Force development was normalized to cross-sectional area and fit to a modified Hill equation: $F/F_{max}= 1 + 10\text{^}[n_H(pCa_{50}\text{-}pCa)]$ where F_{max} is the maximal Ca^{2+} saturated force, F is the steady-state force, n_H is the Hill coefficient, and $pCa = -\log[Ca^{2+}]$; pCa_{50} is the pCa at which F is 50% of F_{max}. ATP consumption was normalized to muscle volume and plotted as function of normalized force obtained at the various $[Ca^{2+}]$ and fit by linear regression to obtain tension-cost, the amount of ATP consumed to maintain a certain level of tension development. For the single myofibril experiments, the rates of the tension increase following a step increase in $[Ca^{2+}]$ (k_{ACT}) or following a rapid release-restretch maneuver (k_{TR}), as well as the fast exponential phase of relaxation (k_{EXP}), were estimated by exponential fit to the data; the rate of the slow phase of relaxation (k_{LIN}) was estimated by linear regression. Data were analyzed using two-way ANOVA. Significance was assumed at $P < 0.05$; data are presented as mean ± S.E.M.

3. Results

3.1. Titin isoform and myofibrillar protein expression profile

Figure 1A shows a typical agarose SDS gel analysis of a rat tibialis anterior muscle (TA). As has been reported previously, wild-type (WT) TA expresses two titin isoforms at ~3.44 MDa and ~3.30 MDa, while homozygous (HM) muscles express the much larger titin isoform at ~3.75 MDa[14]. As is illustrated by the SDS-PAGE analysis of a TA muscle in Figure 1B, overall myofilament protein isoform expression was comparable between Wt and HM TA muscles. Similar data were obtained in TA muscles from 4 separate HM and WT animals. In addition, there were no significant differences in the relative abundance (relative to actin) of the various contractile proteins between the HM and WT groups (data not shown). This finding is consistent with the observation that the stoichiometry of contractile proteins in the striated muscle sarcomere is strictly regulated[26].

3.2. Passive tension development

Fiber bundles and single myofibrils of both WT and HM mutant muscles were stretched over a range of SL's (~2.5 μm to ~4 μm) and passive tension was recorded several seconds following each SL change, that is, at a time when a large component of immediate stress relaxation had dissipated. Passive tension was recorded both in fiber bundles, and in single myofibrils; panel A in Figure 2 illustrates a single myofibril from the WT (top) and HM (bottom), respectively (SL = ~2.8 μm). As illustrated in Figure 2, passive tension was markedly reduced at all sarcomere lengths in both TA bundles (panel B) and single myofibrils (panel C) in HM compared to WT preparations. This significant depression in the passive force-SL relationship in the HM group is consistent with the longer titin isoform (N2BA-G) expressed in HM muscles compared to the shorter N2B skeletal specific isoform expressed in WT muscles (cf. Figure 1).

3.3. Tension & ATPase activity in fiber bundles

Tension development and ATPase activity were measured in fiber bundles of WT and HM TA muscles as illustrated in Figure 3A for a contraction at maximum saturated [Ca^{2+}] and SL = 2.8 μm. Upon activation, tension development (top panel) increases towards steady state concomitant with a reduction in [NADH] (bottom panel) in the measurement chamber, indicative of ATP consumption by active cycling cross-bridges. As this typical example illustrates, both steady state tension and ATP consumption rate were significantly reduced in the HM fiber bundle compared to the WT fiber bundle. That this was the case at all [Ca^{2+}] studied is shown by the force-Ca^{2+} relationships shown in panel B indicating, on average, maximum tension development was ~25% lower in the HM fiber group. Moreover, the entire force-Ca^{2+} relationship was displaced to lower [Ca^{2+}] (~0.06 pCa units) indicating decreased myofilament calcium sensitivity in the HM fiber group. There were no differences in the level of cooperativety, as indexed by the Hill coefficient, between the WT and HM fiber groups.

Maximum ATPase activity was, on average, ~40% lower in the HT fiber group (not shown). Tension-cost, the amount of ATP consumed as a function of tension development over a range of [Ca^{2+}], was on average ~25% lower in the HT group as shown in panel C. This result is consistent with the larger reduction in ATPase activity than tension development indicating a reduction in cross-bridge cycle kinetics[19, 27, 28] in myofilaments containing the mutant larger titin.

3.4. Impact of Sarcomere Length in fiber bundles

Increasing SL from 2.8 μm to 3.2 μm resulted in increased (~10%) maximum tension development (Figure 4A) and significantly increased myofilament Ca^{2+} sensitivity (+0.05 pCa units; Figure 4B) in the WT fiber bundles, consistent with robust myofilament length dependency properties in WT muscles. In contrast, increased SL in HM fiber bundles was associated with a reduced increase in maximum tension (~7.5%) and lack of a significant change in myofilament Ca^{2+} sensitivity (+0.02 pCa units. SL did not affect maximum ATPase activity (figure 4C) in either muscle group, while tension cost (figure 4D) was significantly reduced upon an increase in SL only in the WT muscle group to approach values recorded for the HM muscle at either SL. Thus, myofilament length dependent activation properties were observed in WT fiber bundles, and these properties were significantly blunted in the HM fiber bundles.

3.5. Activation and relaxation kinetics in myofibrils

Activation-relaxation force kinetics were studied in single myofibrils to further assess cross-bridge cycle kinetics. The method is illustrated in Figure 5. Upon rapid solution switch to the activating solution, myofibril tension increases exponentially to reach a steady state at which time a rapid release-restretch maneuver is used to measure tension redevelopment rate, k_{TR}. Upon rapid solution switch back to the relaxation solution, tension relaxes in a biphasic fashion, as has been reported previously[29, 30], first following a close to linear trajectory at a relatively slow rate, followed by a faster exponential phase. This portion of the activation-relaxation cycle is shown more clearly by the expanded traces shown in panel B. Activation (k_{ACT}), $k_{TR}$and the rapid relaxation phase (k_{EXP}) kinetics were estimated by exponential fits to the tension data, while the slow linear relaxation kinetics were estimated by linear regression fit of the tension data. The average fit parameters are summarized in Table 1. As was the case in the multicellular fiber bundles (cf. Figure 4A), maximum tension development was significantly reduced (~25%) in HM compared to WT myofibrils. Moreover, tension development kinetics, for both Ca^{2+} activation (k_{ACT}) and tension redevelopment (k_{TR}), were reduced by ~20% in the HM myofibrils, consistent with the 25% reduction in tension-cost measured in multicellular fiber bundles (cf. Figure 4D). On the

other hand, there were no differences in rate parameters between the WT and HM myofibrils for both the slow linear phase and the faster exponential phase of relaxation. There was a small (~8%), albeit non-significant, decrease in the duration of the linear relaxation phase in the HM myofibrils.

4. Discussion

The purpose of this study was to investigate the consequences of expressing a longer titin isoform on the SL dependence of force production and ATP consumption in rat tibialis anterior (TA) muscle. Previously, to study the effect of titin isoform on striated muscle mechanics it was necessary to use different tissues expressing different titin isoforms. One caveat to this approach, however, is that tissues that naturally express alternative native titin isoforms also contain differences in other major contractile proteins. For instance, in both skeletal and cardiac muscle there is a positive correlation between the MHC isoform expression, the rate of ATP hydrolysis and the length of the titin molecule. This introduces ambiguity in assigning the impact of each individual contractile component on biophysical parameters such as myofilament length dependent activation[31, 32]. Here, we were able to circumvent such confounding factors by using a rat that has an autosomal mutation causing it to differentially express the giant N2BA-G titin isoform. Moreover, the lack of major isoform differences in other contractile proteins between WT and HM in the tibialis anterior muscle (TA; figure 1) raises confidence that chemo-mechanical differences between WT and HM muscle preparations was indeed due to the presence of the longer titin isoform. Nearly all of the passive tension in skeletal muscle is carried by titin. Indeed, the inclusion of the longer titin isoform in HM preparations resulted in much lower passive forces as compared to WT preparations, and is consistent with previously published results (Fig. 2B& C) [15, 17].

Considering that many studies have found correlations between titin isoform length and length dependent activation, a major purpose here was to determine whether muscles harboring a longer titin maintain a similar level of regulation by sarcomere length as muscles from WT rats[6–10]. WT TA tissue displayed length dependency in terms of maximum tension development and Ca^{2+} sensitivity, which was blunted in HM tissue (cf. Figure 4). This result indicates that expression of a longer titin isoform does not eliminate, but rather attenuates LDA. Moreover, HM tissue also exhibited a blunted length dependency of tension cost compared to WT tissue. However, presence of a longer titin isoform did not appear to alter either cooperativity or the force per cross-bridge as indexed by the Hill coefficient and high-frequency muscle stiffness, respectively. Therefore, titin must alter contraction through mechanisms other than cooperativity or the force per cross-bridge.

Our results on isolated TA skeletal muscle are consistent with a recent study on isolated cardiac muscle, where expression of the larger titin molecule in the HM mutant resulted in reduced maximum tension development and cross-bridge cycling rate (indexed by the k_{tr} parameter), and a virtual elimination of myofilament length dependent activation[17]. Preliminary results from our laboratory have confirmed these mechanical observations (data not shown). What may be the mechanisms that result in blunted length dependency? Several potential mechanisms have been proposed to underlie this phenomenon (reviewed in [6]), including modulation of troponin Ca^{2+} affinity, alterations of myosin structure, a modulation of the feedback between attached cross-bridges and thin filament activation status, and spread of cooperative activation[33]. Another mechanism that has been proposed is a direct modulation of myofilament calcium responsiveness due to alterations in inter filament spacing[34]. Indeed, preliminary data shows an expanded myofilament lattice in isolated HM skinned myocardium (data not shown). Hence, although we did not measure inter filament spacing in TA muscles, a similar phenomenon may be present in these muscles

studied here. However, accumulating evidence have shed doubt on the notion that inter filament spacing directly modulates myofilament calcium responsiveness (reviewed in [6]. Rather, an expanded myofilament lattice may be caused by the reduction in titin strain, thereby allowing the filaments to move further apart at any given sarcomere length, while at the same time, a reduction in titin strain may also reduce the impact of titin strain on contractile protein structure such as, for example, troponin and myosin[35, 36].

It should be noted that the RBM20 deficiency that underlies the HM mutation that we studied here affects a multitude of proteins besides the alternative splicing of titin, including Ca^{2+} handling proteins, signal transduction proteins, as well as tropomyosin[16]. In general, Ca^{2+} handling proteins are not expected to affect myofilament function in skinned muscle. Likewise, tropomyosin isoform expression, at least in myocardium, has not been shown to affect maximum force development or tension-cost[37]. The signal transduction protein affected by RBM20 (CamKD) operates mainly in the nucleus, although translocation to the cytosol in HM could have resulted in altered contractile protein phosphorylation, particularly titin. A recent report demonstrates phosphorylation at PKC target site S26 in pathological human skeletal muscle titin, resulting in increased passive tension and myofilament Ca^{2+} responsiveness, but reduced tension-cost and no impact on maximum force development or titin isoform expression[38]. Of note, the changes in myofilament mechanical and energetic parameters and titin isoform observed in the current study are quite distinct, reducing the likelihood that contractile protein phosphorylation changes played a large role in our study. Moreover, no changes in contractile protein phosphorylation, including titin, were noted in a previous study on HM skinned myocardium[17]. Nevertheless, since we did not measure contractile protein phosphorylation in HM and WT TA myofilaments, a role for altered post-translational modification cannot fully be ruled out.

In addition to blunting the influence of length on the regulation of contraction, there was a reduction in overall maximal force, maximal ATP consumption, and tension cost in TA fiber bundles from the HM rats compared to WT. The greater reduction in maximum ATPase (~40%) compared to the decrease in maximal force production (~25%) is in agreement with the overall lower tension cost in the HM tissue (cf Figure 4). Tension cost is related to $g$or the rate by which cross-bridges detach and leave the strong binding state. Based on the Huxley two state cross-bridge model, a reduction in the rate of detachment shifts the equilibrium of cross-bridges from the weakly bound state to the strongly bound state. Because the amount of force a muscle can produce is directly related to the percentage of cross-bridges in the strongly bound, force producing state, a decrease in g is expected to increase maximal force, opposite from what we observed in the present study. Therefore, the effects of a longer titin on cross-bridge kinetics cannot be explained by a simple reduction in the rate of cross-bridge detachment.

To gain further insight into the effect of the titin mutant on force production and cross-bridge kinetics, we additionally examined activation and relaxation kinetics in the single myofibril preparation. Maximum tension developed by a multi-cellular muscle preparation is directly proportional to both cross-sectional area and the density of myofibrils per unit of cross-sectional area[20]. Single myofibrils from HM tissue exhibited a similar decrease in maximal tension production compared to WT myofibrils (Table 1) as we observed in the multi-cellular fiber bundles. Therefore, the reduction in tension development in the HM muscles could not have been the result of a loss of overall contractile machinery, but rather must have been the result of altered contractile protein functional properties. Similar to tension cost, the slope of the initial phase of relaxation in myofibrils (k_{LIN}) and the duration of this phase (t_{LIN}) are thought to reflect the rate of cross-bridge detachment. While there was a trend for a reduction of k_{LIN} in HM myofibrils, this was not statistically significant.

Thus, presence of the mutant titin in the HM myofibrils minimally impacted relaxation kinetics. The rate of force development following either a step-wise increase in [Ca^{2+}] or following a release-restretch maneuver is related to the combined rates of cross-bridge attachment (*f*) and detachment (*g*). Single myofibrils from HM tissue showed a reduction in force development compared to WT myofibrils, suggesting an overall slowing of cross-bridge cycling kinetics. The combination of a decrease in maximal force, a reduction in *g* (measured through tension cost and suggested in single myofibrils) and a reduction in *f+g* (suggested from activation kinetics in single myofibrils) suggests that presence of a longer titin isoform in the sarcomere more strongly influences the apparent rate of cross-bridge attachment (*f*) than it does the apparent rate of detachment (*g*).

One mechanism that might explain why tissue expressing a longer titin isoform would display reduced maximum tension development, calcium sensitivity, and cross-bridge cycling kinetics is related to lattice spacing (reviewed in [39, 40]). The muscle sarcomere maintains nearly a constant volume. Therefore, upon an increase in sarcomere length there is a reduction in muscle width as well as the spacing between the thick and thin filaments[41]. This reduction in sarcomere lattice spacing may increase the probability of a myosin head attaching to actin. Titin is thought to play a role in the reduction of lattice spacing upon an increase in SL since it provides a radial force on the thick and thin filament upon stretch, bringing them closer together. Therefore, a longer titin isoform would be expected to provide less of a radial force, thereby reducing lattice spacing less and subsequently reducing the probability of actin and myosin interaction. This is supported by the observation that specific degradation of titin with trypsin causes a reduction in length dependency concomitant with an increase in lattice spacing[8]. Previous data published from our laboratory, however, have shed doubt on the influence of lattice spacing in LDA, suggesting other mechanisms might be responsible. For instance, rather than only pulling the thick and thin filaments together, the strain produced by titin with an increase in SL is also transmitted lengthwise along the thick and thin filaments, and has been shown to induce geometric rearrangements that favor actin-myosin interaction[35, 42], and that possibly also affects cross-bridge cycle kinetics. Presumably, a longer titin transmits less strain along the thick and thin filaments for a given change in SL and therefore would be expected to have an attenuated response to changes in length, as seen here. Our data showing a reduction in cross-bridge kinetics and length dependency are in agreement with the hypothesis that the presence of a longer titin isoform reduces maximal force, calcium sensitivity and cross-bridge cycling kinetics by reducing the amount of longitudinal strain transmitted along the thick and thin filaments.

Limitations

We studied tension and ATPase activity at short (SL=2.8 μm) and long (SL=3.2 μm). However, single myofibrils were only studied at the short SL (2.8 μm) because large sarcomere inhomogeneity upon rapid activation was observed at the longer SL, precluding assessment of length dependent activation at the single myofibril data. Moreover it should be noted that the fiber bundle experiments were performed at a different temperature than the single myofibril experiments. That is, the ATPase activity of the TA muscle was too slow to be reliably measured at 15 °C, prompting measurement of those data at 20 °C. Single myofibril experiments, on the other hand, could not be conducted at 20 °C due to preparation run-down.

Conclusions

We studied the impact of titin isoform expression on myofilament function in tibialis anterior muscle of the rat. Presence of a longer titin isoform reduced tension development, calcium sensitivity, cross-bridge cycle kinetics, and length dependent activation properties.

We propose that strain transmitted by titin to the contractile apparatus affects cross-bridge cycle kinetics and that this mechanism may underlie length dependent properties of striated muscle.

Acknowledgments

Supported by NIH HL62426, HL07692 and HL075494 (PdT) and HL77196 (MG). We thank Jonathan Pleitner for performing the agarose and polyacrylamide gel electrophoresis.

Cited Literature

1. LeWinter MM, Granzier H. Cardiac titin: a multifunctional giant. Circulation. 2010; 121:2137–2145. [PubMed: 20479164]
2. Voelkel T, Linke WA. Conformation-regulated mechanosensory control via titin domains in cardiac muscle. Pflugers Arch. 2011; 462:143–154. [PubMed: 21347754]
3. Krüger M, Linke WA. The giant protein titin: a regulatory node that integrates myocyte signaling pathways. Journal of Biological Chemistry. 2011; 286:9905–9912. [PubMed: 21257761]
4. Labeit S, Kolmerer B. Titins: giant proteins in charge of muscle ultrastructure and elasticity. Science. 1995; 270:293–296. [PubMed: 7569978]
5. Granzier H, Labeit S. Cardiac titin: an adjustable multi-functional spring. J. Physiol. (Lond.). 2002; 541:335–342. [PubMed: 12042342]
6. de Tombe PP, Mateja RD, Tachampa K, Ait Mou Y, Farman GP, Irving TC. Myofilament length dependent activation. J Mol Cell Cardiol. 2010; 48:851–858. [PubMed: 20053351]
7. Ait Mou Y, le Guennec J-Y, Mosca E, de Tombe PP, Cazorla O. Differential contribution of cardiac sarcomeric proteins in the myofibrillar force response to stretch. Pflugers Arch. 2008; 457:25–36. [PubMed: 18449562]
8. Cazorla O, Wu Y, Irving TC, Granzier H. Titin-based modulation of calcium sensitivity of active tension in mouse skinned cardiac myocytes. Circ Res. 2001; 88:1028–1035. [PubMed: 11375272]
9. Fukuda N, Wu Y, Farman G, Irving TC, Granzier H. Titin isoform variance and length dependence of activation in skinned bovine cardiac muscle. J. Physiol. (Lond.). 2003; 553:147–154. [PubMed: 12963792]
10. Piroddi N, Belus A, Scellini B, Tesi C, Giunti G, Cerbai E, Mugelli A, Poggesi C. Tension generation and relaxation in single myofibrils from human atrial and ventricular myocardium. Pflugers Arch. 2007; 454:63–73. [PubMed: 17123098]
11. Helmes M, Trombitas K, Granzier H. Titin develops restoring force in rat cardiac myocytes. Circ Res. 1996; 79:619–626. [PubMed: 8781495]
12. Greaser ML, Krzesinski PR, Warren CM, Kirkpatrick B, Campbell KS, Moss RL. Developmental changes in rat cardiac titin/connectin: transitions in normal animals and in mutants with a delayed pattern of isoform transition. J. Muscle Res. Cell. Motil. 2005; 26:325–332. [PubMed: 16491431]
13. Warren CM, Krzesinski PR, Campbell KS, Moss RL, Greaser ML. Titin isoform changes in rat myocardium during development. Mech. Dev. 2004; 121:1301–1312. [PubMed: 15454261]
14. Li S, Guo W, Schmitt BM, Greaser ML. Comprehensive analysis of titin protein isoform and alternative splicing in normal and mutant rats. J. Cell. Biochem. 2012; 113:1265–1273. [PubMed: 22105831]
15. Greaser ML, Warren CM, Esbona K, Guo W, Duan Y, Parrish AM, Krzesinski PR, Norman HS, Dunning S, Fitzsimons DP, Moss RL. Mutation that dramatically alters rat titin isoform expression and cardiomyocyte passive tension. J Mol Cell Cardiol. 2008; 44:983–991. [PubMed: 18387630]
16. Guo W, Schafer S, Greaser ML, Radke MH, Liss M, Govindarajan T, Maatz H, Schulz H, Li S, Parrish AM, Dauksaite V, Vakeel P, Klaassen S, Gerull B, Thierfelder L, Regitz-Zagrosek V, Hacker TA, Saupe KW, Dec GW, Ellinor PT, et al. RBM20, a gene for hereditary cardiomyopathy, regulates titin splicing. Nat. Med. 2012; 18:766–773. [PubMed: 22466703]
17. Patel JR, Pleitner JM, Moss RL, Greaser ML. THE MAGNITUDE OF LENGTH-DEPENDENT CHANGES IN CONTRACTILE PROPERTIES VARIES WITH TITIN ISOFORM IN RAT VENTRICLES. AJP: Heart and Circulatory Physiology. 2011

18. de Tombe PP, Stienen GJ. Protein kinase A does not alter economy of force maintenance in skinned rat cardiac trabeculae. Circ Res. 1995; 76:734–741. [PubMed: 7728989]
19. Rundell VLM, Manaves V, Martin AF, de Tombe PP. Impact of beta-myosin heavy chain isoform expression on cross-bridge cycling kinetics. Am J Physiol Heart Circ Physiol. 2005; 288:H896–H903. [PubMed: 15471982]
20. Colomo F, Piroddi N, Poggesi C, te Kronnie G, Tesi C. Active and passive forces of isolated myofibrils from cardiac and fast skeletal muscle of the frog. J. Physiol. (Lond.). 1997; 500(Pt 2): 535–548. [PubMed: 9147336]
21. de Tombe PP, Belus A, Piroddi N, Scellini B, Walker JS, Martin AF, Tesi C, Poggesi C. Myofilament calcium sensitivity does not affect cross-bridge activation-relaxation kinetics. Am. J. Physiol. Regul. Integr. Comp. Physiol. 2007; 292:R1129–R1136. [PubMed: 17082350]
22. Brenner B, Eisenberg E. Rate of force generation in muscle: correlation with actomyosin atpase activity in solution. Proc.Natl.Acad.Sci. 1986; 83:3542–3546. [PubMed: 2939452]
23. Warren CM, Krzesinski PR, Greaser ML. Vertical agarose gel electrophoresis and electroblotting of high-molecular-weight proteins. Electrophoresis. 2003; 24:1695–1702. [PubMed: 12783444]
24. Giulian GG, Moss RL, Greaser M. Improved methodology for analysis and quantitation of proteins on one-dimensional silver-stained slab gels. Anal. Biochem. 1983; 129:277–287. [PubMed: 6189421]
25. Tesi C, Colomo F, Nencini S, Piroddi N, Poggesi C. The effect of inorganic phosphate on force generation in single myofibrils from rabbit skeletal muscle. Biophys. J. 2000; 78:3081–3092. [PubMed: 10827985]
26. de Tombe PP, Solaro RJ. Integration of cardiac myofilament activity and regulation with pathways signaling hypertrophy and failure. Ann Biomed Eng. 2000; 28:991–1001. [PubMed: 11144684]
27. Brenner B. Effect of Ca2+ on cross-bridge turnover kinetics in skinned single rabbit psoas fibers: implications for regulation of muscle contraction. Proc Natl Acad Sci USA. 1988; 85:3265–3269. [PubMed: 2966401]
28. Wannenburg T, Janssen PM, Fan D, de Tombe PP. The Frank-Starling mechanism is not mediated by changes in rate of cross-bridge detachment. Am. J. Physiol. 1997; 273:H2428–H2435. [PubMed: 9374781]
29. Stehle R, Kruger M, Pfitzer G. Force kinetics and individual sarcomere dynamics in cardiac myofibrils after rapid ca(2+) changes. Biophys. J. 2002; 83:2152–2161. [PubMed: 12324432]
30. Tesi C, Piroddi N, Colomo F, Poggesi C. Relaxation kinetics following sudden Ca(2+) reduction in single myofibrils from skeletal muscle. Biophys. J. 2002; 83:2142–2151. [PubMed: 12324431]
31. Cazorla O, Freiburg A, Helmes M, Centner T, McNabb M, Wu Y, Trombitas K, Labeit S, Granzier H. Differential expression of cardiac titin isoforms and modulation of cellular stiffness. Circ Res. 2000; 86:59–67. [PubMed: 10625306]
32. Prado LG, Makarenko I, Andresen C, Kruger M, Opitz CA, Linke WA. Isoform diversity of giant proteins in relation to passive and active contractile properties of rabbit skeletal muscles. J Gen Physiol. 2005; 126:461–480. [PubMed: 16230467]
33. Farman GP, Allen EJ, Schoenfelt KQ, Backx PH, de Tombe PP. The role of thin filament cooperativity in cardiac length-dependent calcium activation. Biophys. J. 2010; 99:2978–2986. [PubMed: 21044595]
34. McDonald KS, Moss RL. Osmotic compression of single cardiac myocytes eliminates the reduction in Ca2+ sensitivity of tension at short sarcomere length. Circ Res. 1995; 77:199–205. [PubMed: 7788878]
35. Farman GP, Gore D, Allen E, Schoenfelt K, Irving TC, de Tombe PP. Myosin head orientation: a structural determinant for the Frank-Starling relationship. AJP: Heart and Circulatory Physiology. 2011; 300:H2155–H2160. [PubMed: 21460195]
36. Hsu H, Ait-Mou Y, Irving TC, de Tombe PP. Structural changes in both the troponin complex and the thick filament may underlie myofilament lngth dependent activation. Biophysical J. 2012 abstract (n.d.).
37. Karam CN, Warren CM, Rajan S, de Tombe PP, Wieczorek DF, Solaro RJ. Expression of tropomyosin-κ induces dilated cardiomyopathy and depresses cardiac myofilament tension by

mechanisms involving cross-bridge dependent activation and altered tropomyosin phosphorylation. J. Muscle Res. Cell. Motil. 2011; 31:315–322. [PubMed: 21221740]

38. Ottenheijm CAC, Voermans NC, Hudson BD, Irving T, Stienen GJM, van Engelen BG, Granzier H. Titin-based stiffening of muscle fibers in Ehlers- Danlos Syndrome. J. Appl. Physiol. 2012; 112:1157–1165. [PubMed: 22223454]
39. Fuchs F, Martyn DA. Length-dependent Ca(2+) activation in cardiac muscle: some remaining questions. J. Muscle Res. Cell. Motil. 2005; 26:199–212. [PubMed: 16205841]
40. Millman BM. The filament lattice of striated muscle. Physiological Reviews. 1998; 78:359–391. [PubMed: 9562033]
41. Irving TC, Konhilas J, Perry D, Fischetti R, de Tombe PP. Myofilament lattice spacing as a function of sarcomere length in isolated rat myocardium. Am J Physiol Heart Circ Physiol. 2000; 279:H2568–H2573. [PubMed: 11045995]
42. Mateja RD, de Tombe PP. Myofilament Length-Dependent Activation Develops within 5 ms in Guinea-Pig Myocardium. Biophys. J. 2012; 103:L13–L15. [PubMed: 22828350]

Highlights

- Myofilament length dependent activation (LDA) underlies the Starling Law of the heart.
- The giant molecule titin may play a pivotal role in length dependency.
- We studied striated muscle from mutant and wild-type rats with varied titin lengths.
- Long Titin was associated with altered LDA.
- Conclusion, titin mediates the length signal so as to modulate LDA.

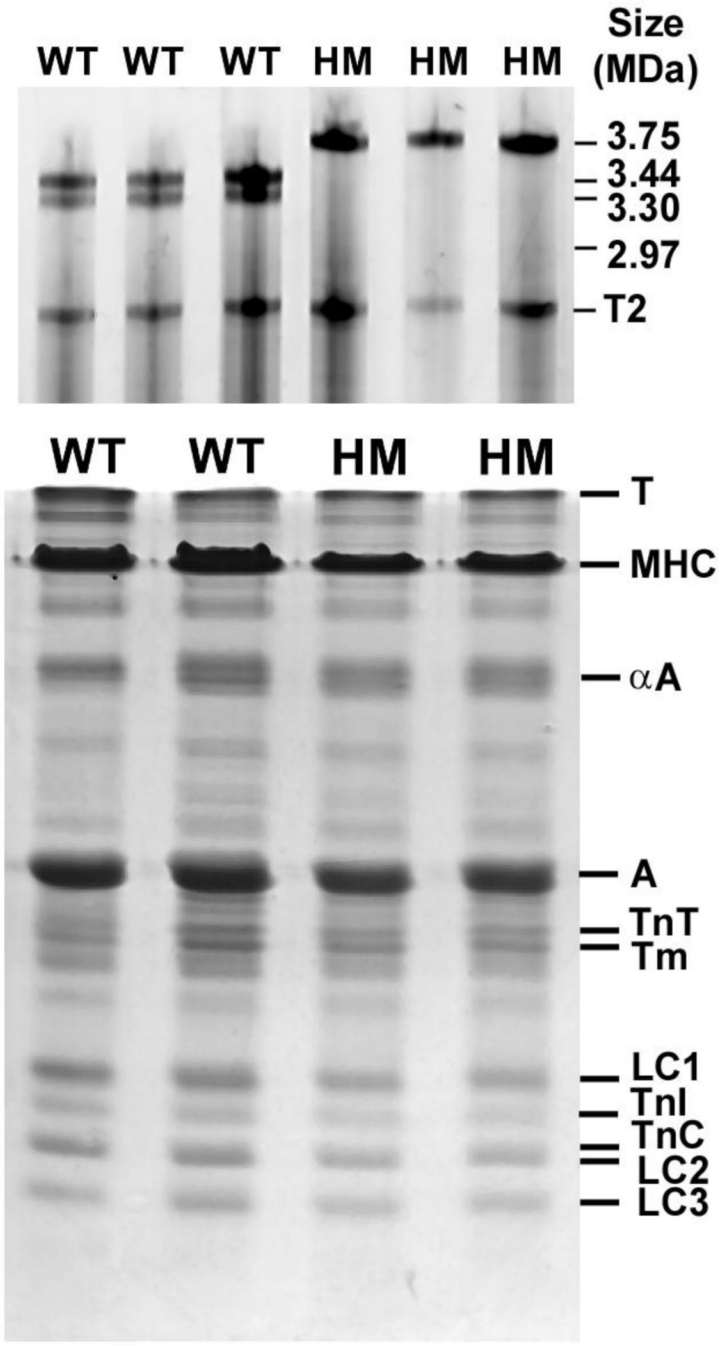

Fig. 1. Protein isoform composition SDS-PAGE analysis

Tibialis anterior skeletal muscle (TA) was harvested from wild type (WT) and homozygous mutant (HM) rats. Top panel: shows agarose gel electrophoresis images used to analyze to titin isoform patterns. HM TA muscle expresses a single titin isoform that is significantly larger than the two major isoforms expressed in wild type TA muscle. T2 is a titin breakdown product which was similar in size between the WT and HM muscles. Bottom panel: myofilament contractile proteins were analyzed by standard 12% SDS-PAGE. There were no significant differences in contractile protein expression between WT and HM muscle. T, titin; MHC, myosin heavy chain; α-A, alpha actinin; A, actin; TnT, troponin T;

Tm, tropomyosin; LC1, myosin light chain 1; TnI, troponin I; TnC, troponin C; LC2, myosin light chain 2; LC3, myosin light chain 3.

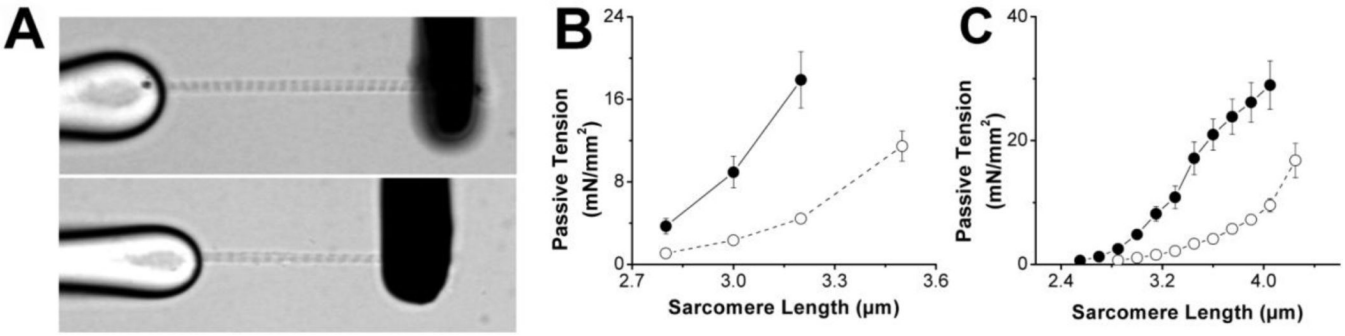

Fig. 2. Passive Tension

Panel A shows a single myofibril from a WT (top) and HM (bottom) TA muscle (SL=2.8 μm). Myofibrils were attached to a stiff glass micropipette (left) and a flexible thin glass micropipette (coated with blank ink to improve contrast; right); deflection of the black pipette was used to estimate myofibril force development. Passive tension measured as function of SL is shown for single myofibrils in panel B and fiber bundles in panel C. Passive muscle force was significantly higher in WT (solid lines and filled symbols) compared to HM (dashed line and empty symbols) TA preparations.

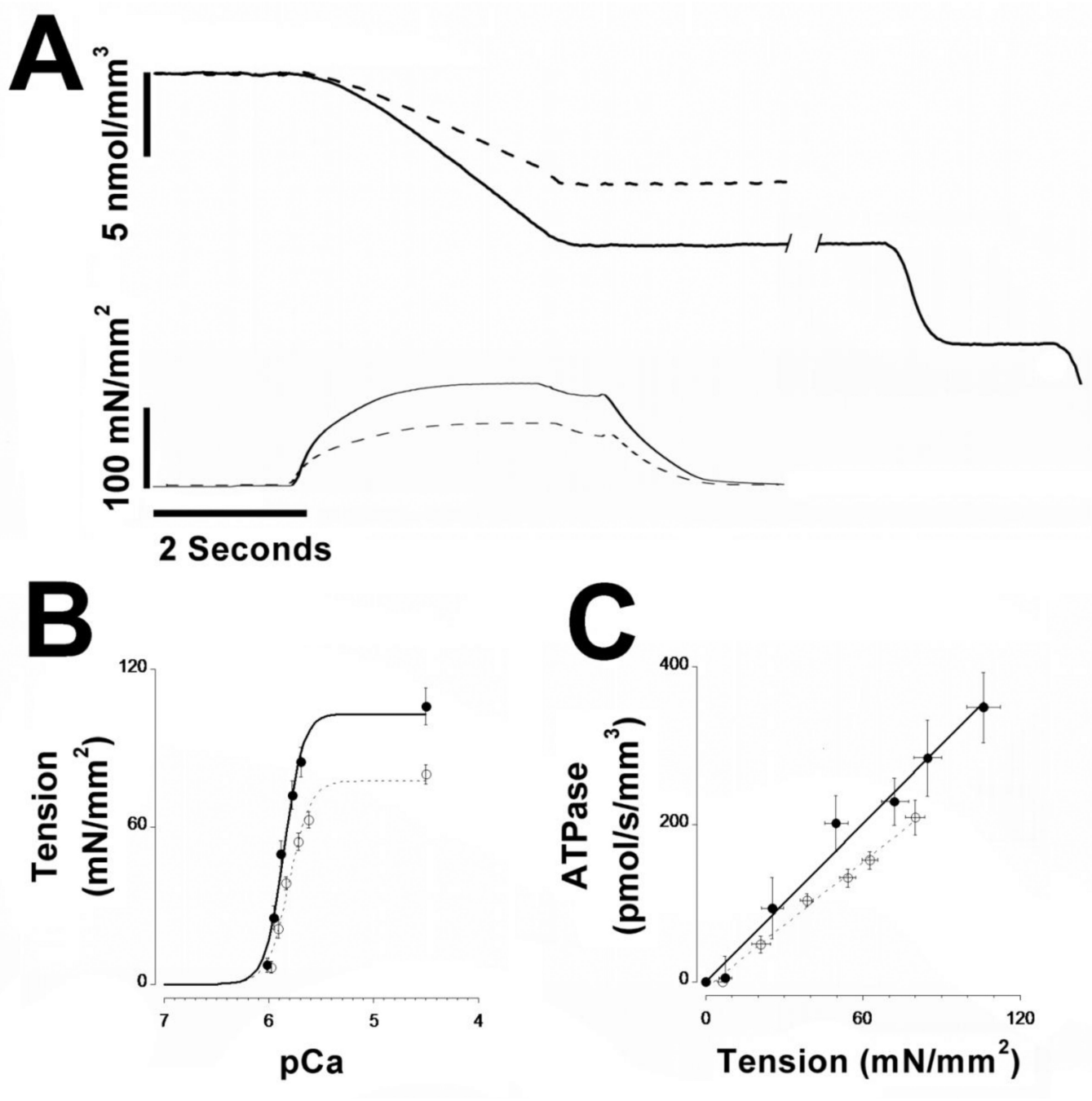

Fig 3. Tension development, ATPase activity, and tension-cost in fiber bundles

Multi-cellular skinned fiber bundles were prepared from WT (solid line and closed symbols) and HM (dashed line and open symbols). Panel A shows typical recordings of [NADH] (top trace) and tension development (bottom trace). Upon activation of the fiber bundle, tension develops concomitant with reduction of [NADH], indicative of increased ATPase activity by the muscle. Following removal of the fiber bundle from the measurement chamber, [NADH] is calibrated by repeated injections of 500 pmol ADP (shown at the right for the WT trace only). Panel B shows average tension-Ca^{2+} relationships (filled symbols are WT; empty symbols are HM), while panel C shows average tension-ATPase relationships obtained in the WT and HM fiber bundles (filled symbols are WT; empty symbols are HM). HM fiber

bundles exhibited reduced tension development, myofilament Ca^{2+} sensitivity, and tension-cost. Temperature, 20 °C; SL=2.8 μm.

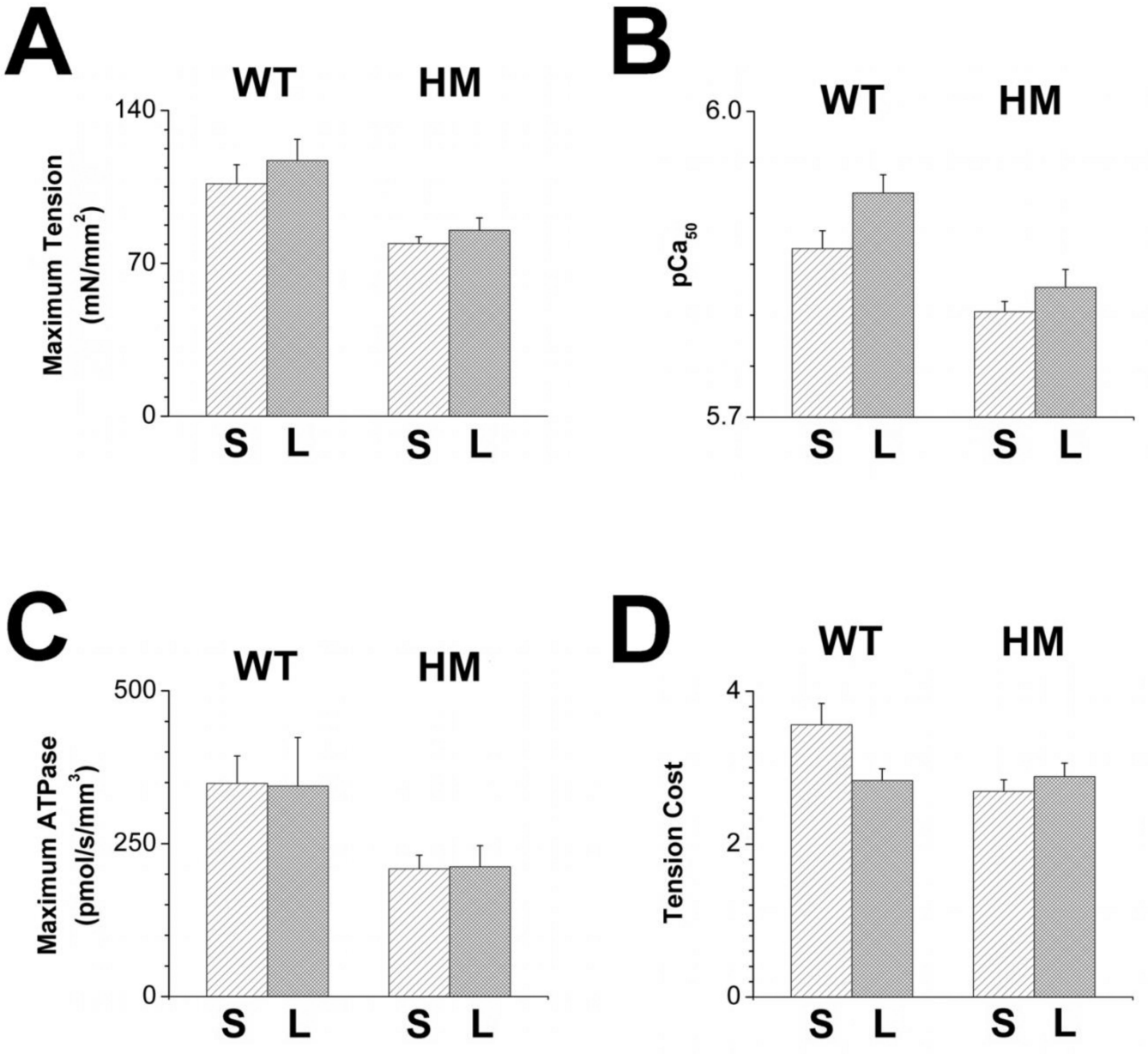

Fig. 4. Impact of sarcomere length

Tension-Ca^{2+} and tension-ATPase relationship were measured in WT (light bars) and HM (dark grey bars) fiber bundles at short (S, SL=2.8 μm) and long (L, SL=3.2 μm) sarcomere length. Maximum tension (panel A), calcium sensitivity (panel B), maximum ATPase (panel C) and tension-cost (panel D) were reduced in HM compared to WT fiber bundles at short and long SL. Presence of the shorter isoform in the WT fiber bundles was associated with robust myofilament length dependent activation of maximum tension, calcium sensitivity, and tension-cost that was blunted in the HM fiber bundles.

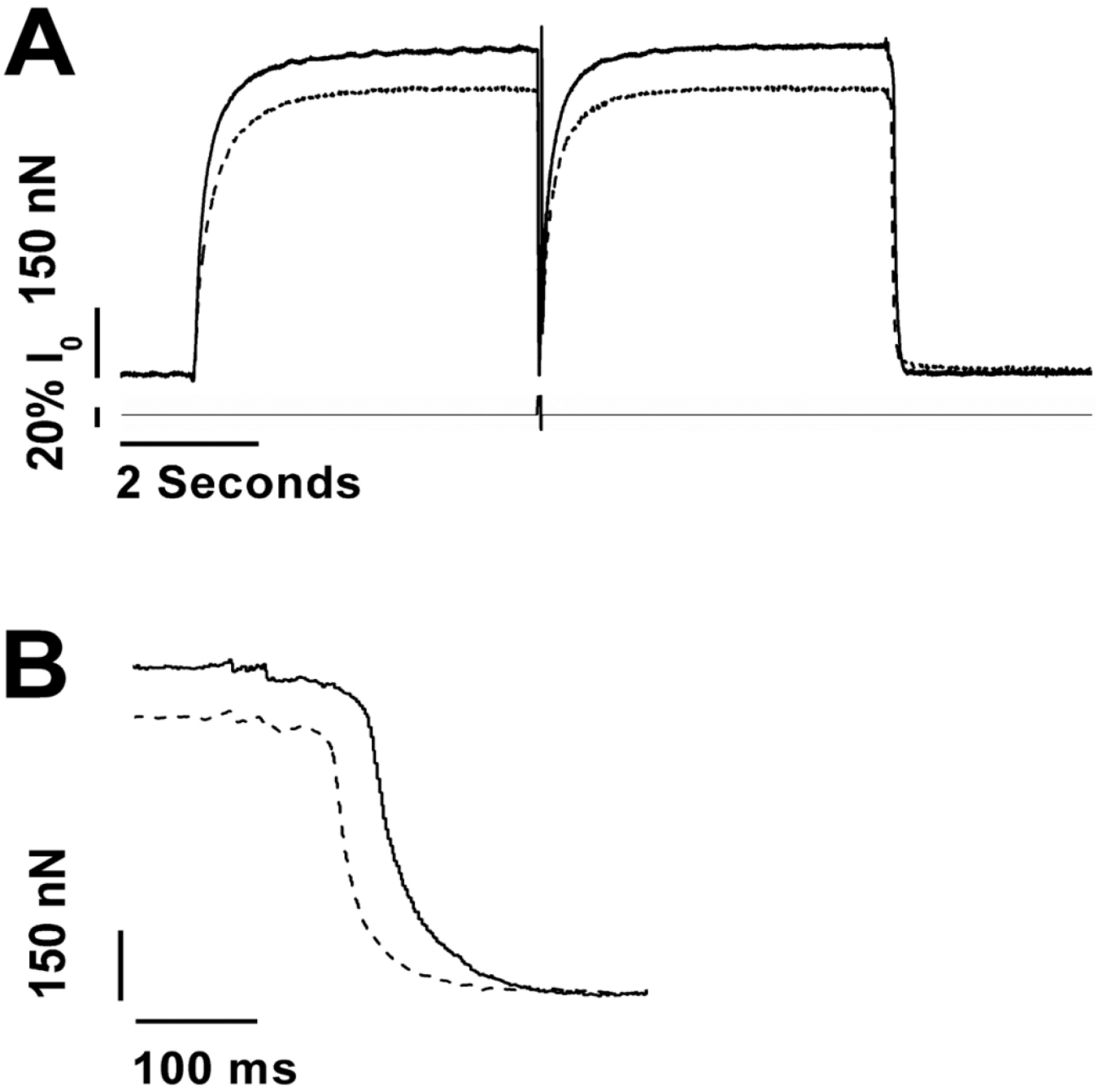

Fig. 5. Activation-relaxation kinetics by fast solution switch in single myofibrils

Panel A shows typical tension recordings from an activation/relaxation cycle in wild type (solid line) or homozygote mutant (dashed line) TA single myofibrils. Upon Ca^{2+} activation, tension increased exponentially towards steady state, at which time a quick release-restretch protocol (20% muscle length) was employed to assess exponential tension redevelopment rate. Upon rapid removal of activating Ca^{2+}, tension relaxation follows a biphasic pattern as illustrated by the expanded traces in panel B. HM myofibrils displayed reduced maximum tension and reduced activation kinetics. Calibration as indicated; see text for details. Temperature 15 °C; SL = 2.8 μm.

Table 1

Average single myofibril parameters.

	maximum tension (mN/mm^2)	k_{ACT} (s^{-1})	k_{TR} (s^{-1})	k_{LIN} (s^{-1})	t_{LIN} (ms)	k_{EXP} (s^{-1})
WT	110 ± 10	3.26 ± 0.16	4.07 ± 0.16	2.44 ± 0.18	130 ± 10	31 ± 2.0
HM	80 ± 10 *	2.64 ± 0.24 *	3.30 ± 0.27 *	2.40 ± 0.14	120 ± 10	34 ± 4.7

Activation/relaxation tension kinetic parameters were obtained in wild type (WT) and homozygous mutant (HM) single myofibril preparations by rapid solution switching. Ca^{2+} activation was mono-exponential (k_{ACT}), while relaxation was biphasic characterized by a slow linear relaxation phase (rate, k_{LIN}; duration, t_{LIN}) followed by rapid exponential tension decline (k_{EXP}) towards baseline. When tension development had reached steady state (cf. Figure 5), a rapid release-restretch maneuver was employed to measure exponential tension redevelopment (k_{TR}). HM myofibrils displayed reduced maximum tension development and reduced activation kinetics.

Values are expressed as means ± S.E.M.

* $P<0.05$